

# Impurity Conduction and Magnetic Polarons in Antiferromagnetic Oxides

C. Chiorescu and J. L. Cohn

Department of Physics, University of Miami, Coral Gables, Florida 33124

J. J. Neumeier

Department of Physics, Montana State University, Bozeman, Montana 59717

Low-temperature transport and magnetization measurements for the antiferromagnets  $\text{SrMnO}_3$  and  $\text{CaMnO}_3$  identify an impurity band of mobile states separated by energy from electrons bound in Coulombic potentials. Very weak electric fields are sufficient to excite bound electrons to the impurity band, increasing the mobile carrier concentration by more than three orders of magnitude. The data argue against the formation of self-trapped magnetic polarons (MPs) predicted by theory, and rather imply that bound MPs become stable only for  $k_B T$ .

PACS numbers: 75.47.Lx, 72.20.-i, 71.55.-i, 71.27.+a, 75.50.Ee

An electron in a magnetic solid can perturb local moments via exchange interactions between its spin and those of the ions, forming a self-trapped or bound magnetic polaron (MP). Though these concepts were formulated long ago [1], experimental understanding and theoretical development of MP physics have been limited by the relatively small number of materials found to manifest MPs. More recently, renewed interest in the MP problem has been stimulated by studies of carrier-doped antiferromagnetic (AF) manganites [2] and dilute magnetic semiconducting oxides [3]. An important emerging issue for both classes of compounds is the energy position of donor levels (e.g., associated with oxygen vacancies and/or impurities) within the band gap and the contribution of donor-bound charge to MP formation.

Perhaps the simplest AF systems for examining such issues are the nominally  $\text{Mn}^{4+}$  compounds,  $\text{CaMnO}_3$  (CMO) and  $\text{SrMnO}_3$  (SMO) which have a bipartite (G-type) AF ground state and are free from the complex collective interactions of Jahn-Teller-active  $\text{Mn}^{3+}$  ions that characterize more widely studied  $\text{LaMnO}_3$ . They are model systems for MP studies since the couplings between electronic, lattice, and spin degrees of freedom for light electron doping are known [4, 5]. Magnetization [6] and scattering [7] studies imply the existence of MPs in the ground state of CMO when electron doped with La, and theory [4, 5] predicts these electrons form self-trapped MPs, i.e. those bound solely by magnetic exchange interactions with ionic spins. However, shallow impurity states associated with oxygen vacancies are ubiquitous in oxides, and their influence on the energetics of MP formation has received little attention.

Here we report low-temperature transport and magnetic studies on CMO and SMO which reveal surprising features of the donor electronic structure that offer new insight into MP formation in oxides. These compounds are naturally electron doped by low levels of oxygen vacancies ( $n \sim 10^8 - 10^9 \text{ cm}^{-3}$ ) so that the conventional picture of donor-bound electrons in small-radius states predicts insulating behavior at low temperatures. In-

stead, we find that the low- $T$  transport involves an impurity band of mobile electronic states separated by energy from electrons bound in Coulombic potentials. Very weak electric fields ( $E \sim 50 \text{ V/cm}$ ) are sufficient to excite bound electrons to the impurity band, increasing the mobile carrier concentration by more than three orders of magnitude. The data argue against the presence of self-trapped MPs in these compounds and we attribute the onset of a FM contribution to the low- $T$  magnetization of SMO [8] to bound MPs which become stable only for  $k_B T$ . The observations suggest that the tunable mobile carrier density characteristic of the present compounds might be observed and exploited in related compounds for novel studies of correlated electrons.

The synthesis procedures for the single-crystal of  $\text{CaMnO}_3$  (CMO) and polycrystalline specimen of  $\text{SrMnO}_3$  (SMO) are described elsewhere [6, 8, 9, 10]. The net electron densities determined from Hall measurements at room temperature were  $n_H = N_D - N_A \approx 6 \times 10^8 \text{ cm}^{-3}$  (CMO) and  $3 \times 10^8 \text{ cm}^{-3}$  (SMO). These correspond to  $10^3 - 10^4$  electrons per formula unit, attributable to a very small oxygen deficiency. Compensating impurities (e.g. from ppm levels in the starting chemicals) are typical in oxides; the  $T = 300 \text{ K}$  thermopowers [11] of  $-420 \text{ V/K}$  (CMO) and  $-180 \text{ V/K}$  indicate a greater compensation in SMO. The dc resistivity and Hall coefficient were measured in a 9-T magnet on 6-probe specimens with silver paint contacts. Magnetic field was applied perpendicular to the plane of plate-like specimens in which dc currents (5 nA to 10 mA) were applied. Both current and field reversal were employed for Hall and magnetoresistance measurements. A thermocouple attached to each specimen monitored temperature rises due to self-heating, observed only at the highest currents employed. Magnetization measurements were performed in a Quantum Design PPM S.

CMO and SMO are orthorhombic and cubic, respectively, with [12]  $T_N \approx 125$  and  $230 \text{ K}$ . They are weakly ferromagnetic (FM) [6, 8] at low  $T$ , with saturation magnetizations  $0.02 - 0.03 \mu_B/\text{Mn ion}$ , but the FM moment

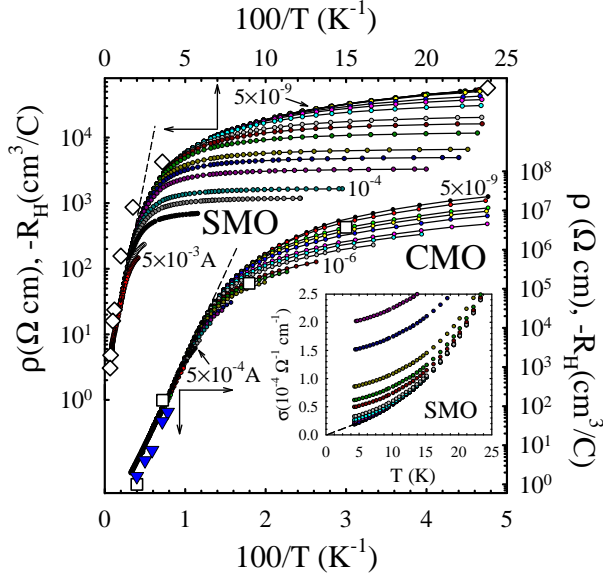


FIG. 1: (Color online)  $\rho$  vs.  $100/T$  for SMO (upper abscissa, left ordinate) and CMO (lower abscissa, right ordinate). Each curve was measured with a different dc current, some of which are labeled; increases are in steps of 1, 3, 5 per decade. Dashed lines are linear fits. Hall coefficients (open squares and diamonds) were measured at the lowest currents. Inverted triangles are Hall data for polycrystalline CMO from Ref. 9. Inset:  $\sigma(T)$  for SMO at various currents (some omitted for clarity).

develops abruptly at  $T < T_N$  for CMO and gradually [8] at  $T \sim 80 \text{ K} \sim T_N$  for SMO. The latter behavior appears to be associated with FM polarons [7], whereas the former may be attributed to an additional FM contribution in CMO from Dzyaloshinsky-Moriya coupling (allowed by symmetry). These materials exhibit band-like, large-polaron transport with mobilities  $\sim 1 \text{ cm}^2/\text{V s}$  at  $T \sim T_N$  [9, 13], which contrasts with the small polaronic character of the paramagnetic phase of hole-doped manganites [14].

Figure 1 shows resistivity data (in zero magnetic field), plotted versus inverse temperature, illustrating the sensitivity of the charge transport in these materials to applied current ( $I$ ) at low  $T$  where impurity conduction is predominant. Several curves for each specimen are labelled by values of  $I$ ; successive curves represent current increases in steps of 1, 3, 5 per decade. This phenomenon is the central focus of this work.

The high- $T$  resistivity has an activated form,  $\rho \propto \exp(\rho_0/k_B T)$ , with  $\rho_0 = 86 \text{ meV}$  and  $25 \text{ meV}$  for CMO and SMO, respectively (dashed lines, Fig. 1). The Hall coefficients ( $R_H$ ) measured at the lowest currents (squares and diamonds, Fig. 1) follow  $\rho(T)$  in their temperature variation, consistent with thermal activation of electrons from donor levels [15] to the conduction band and a weakly  $T$ -dependent mobility. Both  $\rho$  and  $R_H$  become weakly  $T$ -dependent in the impurity conduction regime at the lowest  $T$ , but  $R_H$  does not exhibit the maxi-

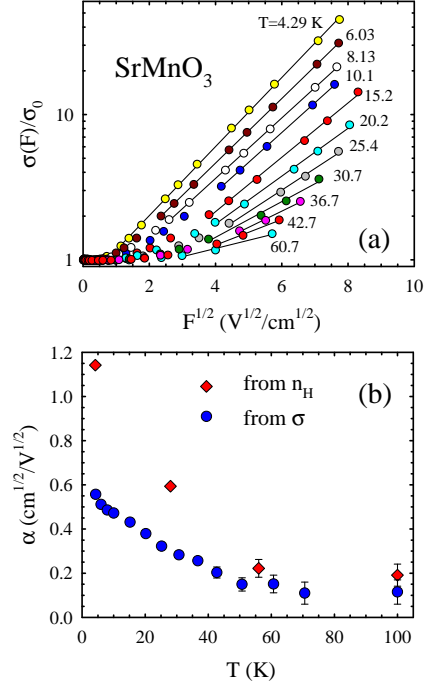


FIG. 2: (Color online) (a) Semilog plot of  $\sigma(F)/\sigma_0$  vs.  $F^{1/2}$  for SMO at various temperatures. Solid lines are linear fits. (b) Slopes  $\alpha$ , determined from (a) (solid circles) and from a similar analysis of the Hall density (Fig. 4).

mum characteristic of a transition to "metallic" in purity-band conduction. This suggests that only a small fraction of bound carriers at low- $T$  are sufficiently mobile to contribute to  $R_H$ . The conductivity ( $\sigma$ ) extrapolates to zero as  $T \rightarrow 0$  for the lowest current (dashed line in inset, Fig. 1), but  $\sigma(T \rightarrow 0)$  for higher currents is finite, indicating that the material is not strictly insulating.

Isothermal measurements of  $\sigma$  vs. applied current density ( $J$ ) indicate that in the non-Ohmic regime  $\sigma$  scales with the transport electric field ( $F = J$ ) as,  $\sigma(F) = \sigma_0 / \exp(-F/F_0)$ , where  $\sigma_0$  ( $I = 5 \text{ nA}$ ). This is shown for SMO in Fig. 2 (a). The temperature dependence of the parameter  $F_0$ , determined from least-squares fits [solid lines, Fig. 2 (a)], is plotted in Fig. 2 (b). This dependence of  $F_0$  on  $T$  is that prescribed by Poole-Frenkel field-assisted ionization [16, 17] of carriers bound to donors, and is discussed in more detail below. Note that  $F_0$  was found to be independent of applied magnetic field up to 9 T in spite of a modest magneto-resistivity, e.g.  $F_0 = 0.13$  and  $0.04$  for  $I = 5 \text{ nA}$  and  $0.5 \text{ mA}$ , respectively, at  $T = 28 \text{ K}$  for SMO. Heating of the sample can be ruled out as the cause of the  $F$  dependence because specimen temperature was monitored directly with a thermocouple, was limited to  $\sim 2-3 \text{ K}$  at the highest current for each temperature, and was corrected for by interpolation on the  $\rho(T)$  curves at fixed  $I$ . Qualitatively similar results have been observed for these same specimens after annealing to vary their oxygen content, and for polycrystalline CMO and  $\text{Ca}_{0.75}\text{Sr}_{0.25}\text{MnO}_3$  [11].

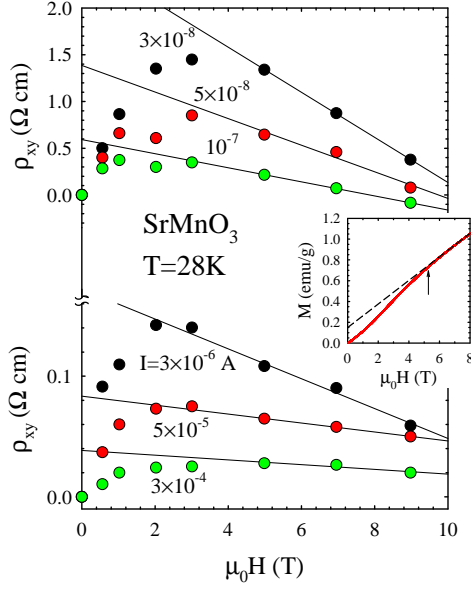


FIG. 3: (Color online) Hall resistivity vs. magnetic field for SM O at  $T = 28$  K. Different curves are labeled by the applied current. The solid lines are linear fits at the highest fields used to determine the normal Hall contribution. The inset shows the magnetization at the same temperature (solid curve) and linear fit to the high-field data (dashed line).

The current and magnetic field dependencies of the Hall resistivity,  $\rho_{xy}$  (Fig. 3), provide further evidence that Poole-Frenkel ionization of trapped carriers underlies the non-Ohmic behavior of . This plot shows  $\rho_{xy}$  vs. magnetic field for SM O at  $T = 28$  K for several values of the applied current. With increasing field,  $\rho_{xy}$  for each current increases to a maximum near  $\mu_0 H \approx 3$  T, and becomes linear in field for  $\mu_0 H \gtrsim 5$  T. This behavior indicates a sum of (positive) anomalous and (negative) normal Hall contributions, consistent with the magnetization (inset, Fig. 3) which exhibits a small FM contribution superposed with the linear AF background. The FM component saturates for  $\mu_0 H \gtrsim 5$  T, and the magnetization becomes linear in field (dashed line) in the same field range as does  $\rho_{xy}$ . The normal Hall coefficient was determined from the high-field slopes,  $R_H = d\rho_{xy}/d(\mu_0 H)$  (solid lines, Fig. 3). Both  $R_H$  and the anomalous contribution to  $\rho_{xy}$  (intercept of solid lines) decrease systematically with increasing current, signaling an increase in the mobile carrier density.

Figure 4 shows the Hall carrier density,  $n_H = 1/(R_H e)$ , plotted versus  $F^{1/2}$  for CM O (lower abscissa, right ordinate) and for SM O (upper abscissa, left ordinate) at several temperatures. The ionization rate in the Poole-Frenkel model [16, 17] incorporates thermal activation as well as field-induced barrier lowering. At low  $T$  where the majority of electrons are trapped, the Hall density should be of the form,  $n_H(F) = N^0 \exp[-(E_b/k_B T - eF^{1/2})]$ , where  $N^0$  is the density of neutral donors and  $E_b$  is the barrier height. The scale for barrier lowering is set by

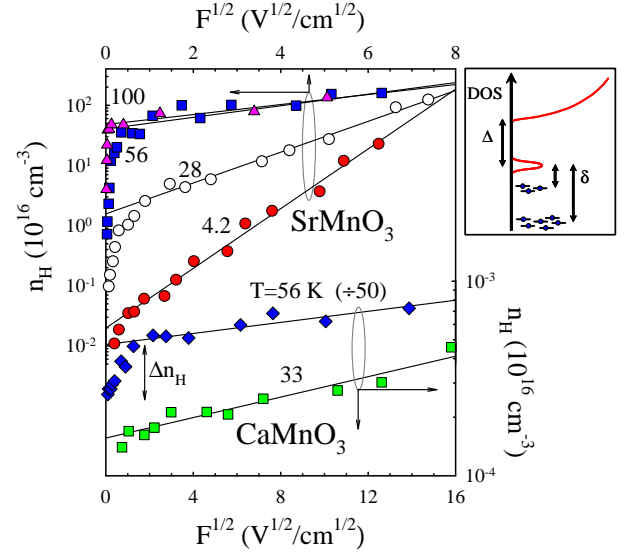


FIG. 4: (Color online) Semilog plots of Hall carrier density vs.  $F^{1/2}$  at different temperatures for CM O (lower abscissa, right ordinate) and SM O (upper abscissa, left ordinate). Solid lines are linear fits. Inset: energy band scheme implied by the temperature and electric-field dependence of  $n_H$  (see text).

$= k_B T$ , where  $E_b = (Ze^3/4\epsilon_0\epsilon_r)^{1/2}$  and  $\epsilon_r$  is an effective relative dielectric constant, often taken to be the high-frequency (optical) value. The low- $T$  values of  $E_b$  determined from the slopes of linear least-squares fits (solid lines, Fig. 4) imply  $E_b \approx 0.2$  meV  $\text{cm}^{1/2}/\text{V}^{1/2}$  (CM O) and  $0.4$  meV  $\text{cm}^{1/2}/\text{V}^{1/2}$  (SM O), in reasonable accord with the value  $0.34$  meV  $\text{cm}^{1/2}/\text{V}^{1/2}$  ( $0.48$  meV  $\text{cm}^{1/2}/\text{V}^{1/2}$ ) estimated for manganites using  $Z = 2$  ( $Z = 1$ ), for singly- (doubly-) occupied vacancies, and  $\epsilon_r \approx 5$  [18].

A compelling feature of the  $n_H(F)$  data is that at each temperature,  $n_H$  extrapolates toward the value  $n_H(300 \text{ K})$ , the latter presumably reflecting nearly full ionization of donors to the conduction band. This implies that all carriers are bound in Coulomb potentials in the ground state, and thus argues strongly against the existence of self-trapped magnetic polarons in this material. The  $n_H(F)$  data for CM O show a much weaker field effect, consistent with the smaller influence of  $F$  on the resistivity (Fig. 1). The difference in the magnitude of the field effect for the two compounds implies a difference in the potential barrier for donor ionization,  $E_b$ . Applying the expression for  $n_H$  above to the low- $T$   $n_H$  data, with  $N^0 = N_D - N_A - n_H(300 \text{ K})$ , yields  $E_b \approx 41$  meV and  $3.5$  meV for CM O and SM O, respectively. We conclude that electrons are not ionized to the conduction band (requiring energy  $E_b$ ), but are rather excited to a band of more mobile impurity states responsible for the low- $T$  conduction, as depicted in the inset of Fig. 4.

Differing local environments, e.g. associated with vacancy clusters or vacancy-acceptor pairs [19], are expected to result in multiple bound-state energies. With increasing  $T$  electrons with larger binding energies are

promoted to the impurity band and rendered mobile in applied field  $F$  so that the  $n_H(F;T)$  data provide for impurity-level spectroscopy. The  $n_H(F)$  curves for SMO at 28 K, 56 K, and 100 K imply  $\sim 14$ – $3$  meV, indicating that there are principally two such bound-state energies (inset, Fig. 4). The larger values of  $\epsilon$  and  $\mu$  for CMO suggest an intrinsic origin (e.g. the buckled Mn-O-Mn bond), but compensation may also play a role.

Two aspects of the data indicate a strong electric-field dependence of the Hall mobility. A low-field increase in the carrier density, designated  $n_H$  in Fig. 4 (vertical arrows), comes to predominate in the total field effect as  $T$  increases. We attribute it to carriers thermally excited to the impurity band where they are more loosely bound and mobile at low fields. This field regime corresponds to Ohmic behavior in Fig. 2, and thus implies  $n_H \propto n_H^1$ . At higher fields within the Poole-Frenkel ionization regime, the values of  $\mu$  for SMO determined from  $(F)$  are substantially lower than those determined from  $n_H(F)$  [Fig. 2 (b)], by an amount that grows with decreasing  $T$  at  $T \sim 60$  K. At 4.2 K,  $n_H \propto F^{1/2}$ , implying  $\mu \propto n_H^{-1/2}$ . These observations suggest interesting correlation effects in the carrier dynamics.

It is likely that transport in the impurity band involves next-nearest-neighbor Mn  $e_g$  orbitals given that nearest-neighbor hopping in the G-type AF lattice is strongly inhibited by Hund's rule. This band may involve excited impurity states since little overlap is to be expected between bound states with a mean spacing  $d \sim 2\beta = 4(N_D - N_A)^{1/3} \sim 60$ – $80$  Å, and radius  $\sim 8$ – $10$  Å (estimated from the donor polarizability [10]).

Though self-trapped MPs appear to be ruled out by our data, the observation that a FM contribution to the magnetization in SMO develops only below  $\sim 80$  K [8], is consistent with bound MP formation for  $k_B T \sim 80$  K. It is plausible that MP de-trapping in electric field locally depolarizes a number of Mn spins. The impurity-band carrier mobility may thus be influenced by changes in both magnetic and Coulomb interactions associated with de-trapping.

In summary, transport measurements in G-type antiferromagnetic perovskite manganites indicate the presence of a mobile band of impurity states to which electrons, bound at energy  $\epsilon$  below  $\mu$ , are excited through barrier-lowering in weak electric fields. The data argue against the formation of self-trapped MPs as predicted by theory, but are consistent with bound MPs that become stable only for  $k_B T \sim 80$  K. Such an impurity band, derived from states involving oxygen vacancies, is likely common to related oxides where similar features in the transport might be observed. Such measurements can be employed as a tool for impurity-level spectroscopy and for studying correlated electrons with a tunable mobile carrier density.

The authors acknowledge helpful comments from S. Satpathy. This material is based upon work supported by the National Science Foundation under grants DMR-0072276 (Univ. Miami) and DMR-0504769 (Mont. St. Univ.), and the Research Corporation (Univ. Miami).

- 
- [1] E. L. Nagaev, Zh. Eksp. Teor. Fiz. Pis'ma Red. 6, 484 (1967) [JETP Lett. 6, 18 (1967)]; T. Kasuya, A. Yanase, and T. Takeda, Sol. St. Commun. 8, 1543 (1970); A. Mauger and D. L. Mills, Phys. Rev. B 31, 8024 (1985); L. Liu, Phys. Rev. B 37, 5387 (1988).
  - [2] See, e.g., Colossal Magnetoresistance, Charge Ordering and Related Properties of Manganese Oxides, edited by C. N. R. Rao and B. Raveau (World Scientific, Singapore, 1998); E. Dagotto, Nanoscale Phase Separation and Colossal Magnetoresistance, Springer Series in Solid-State Sciences, (Springer-Verlag, Berlin, 2003), Vol. 136.
  - [3] C. Liu et al., J. Mater. Sci.: Mater. Electron. 16, 555 (2005); J. M. Coey et al., Nat. Mater. 4, 173 (2005); K. R. Kittilstved et al., Phys. Rev. Lett. 97, 037203 (2006).
  - [4] Y.-R. Chen, and P. B. Allen, Phys. Rev. B 64, 064401 (2001).
  - [5] H. Meskinen, T. Saha-Dasgupta, and S. Satpathy, Phys. Rev. Lett. 92, 056401 (2004); H. Meskinen and S. Satpathy, J. Phys.: Condens. Matter 17, 1889 (2005).
  - [6] J. J. Neumeier and J. L. Cohn, Phys. Rev. B 61, 14319 (2000).
  - [7] E. Granado et al., Phys. Rev. B 68, 134440 (2003).
  - [8] O. Chmaissem et al., Phys. Rev. B 64, 134412 (2001).
  - [9] J. L. Cohn, C. Chiorescu, and J. J. Neumeier, Phys. Rev. B 72, 024422 (2005).
  - [10] J. L. Cohn, M. Peterca, and J. J. Neumeier, Phys. Rev. B 70, 214433 (2004).
  - [11] C. Chiorescu, J. L. Cohn, and J. J. Neumeier, unpublished.
  - [12] E. O. Wollan and W. C. Koehler, Phys. Rev. 100, 545 (1955).
  - [13] C. Chiorescu, J. J. Neumeier, and J. L. Cohn, Phys. Rev. B 73, 014406 (2006).
  - [14] M. Jaime et al., Phys. Rev. Lett. 78, 951 (1997); J. M. De Teresa et al., Phys. Rev. B 58, R5928 (1998); J. L. Cohn, J. Supercond.: Incorp. Nov. Magn., 13, 291 (2000).
  - [15] The calculated band gaps are 0.4 eV and 0.3 eV for CMO and SMO, respectively. See, e.g., W. E. Pickett and D. J. Singh, Phys. Rev. B 53, 1146 (1996) and R. S. Deria et al., Phys. Rev. B 74, 144102 (2006).
  - [16] J. Frenkel, Phys. Rev. 54, 647 (1938).
  - [17] J. G. Simmons, Phys. Rev. 155, 657 (1967); J. L. Hartke, J. Appl. Phys. 39, 4871 (1968); J. R. Yeager and H. L. Taylor, ibid. 39, 5600 (1968); G. A. Dussel and K. W. Boer, Phys. Stat. Sol. 39, 375 (1970).
  - [18] A. S. Alexandrov and A. M. Bratkovsky, J. Phys.: Condens. Matter 11, L531 (1999).
  - [19] B. I. Shklovskii and A. L. Efros, Electronic properties of doped semiconductors, (Springer-Verlag, New York, 1984).